

# Broad-Spectrum G Protein–Coupled Receptor Antagonist, [D-Arg<sup>1</sup>, D-Trp<sup>5,7,9</sup>,Leu<sup>11</sup>]SP: A Dual Inhibitor of Growth and Angiogenesis in Pancreatic Cancer

Sushovan Guha,<sup>1,2</sup> Guido Eibl,<sup>2,4</sup> Krisztina Kisfalvi,<sup>1,2</sup> Robert S. Fan,<sup>1,2</sup> Marie Burdick,<sup>3</sup> Howard Reber,<sup>4</sup> Oscar J. Hines,<sup>4</sup> Robert Strieter,<sup>2,3</sup> and Enrique Rozengurt<sup>1,2</sup>

<sup>1</sup>Department of Medicine, Division of Digestive Diseases, and Molecular Biology Institute; <sup>2</sup>Center for Ulcer Research and Education: Digestive Diseases Research Center, <sup>3</sup>Department of Medicine, Division of Pulmonary and Critical Care Medicine, and <sup>4</sup>Department of Surgery, Section of Gastrointestinal Surgery, David Geffen School of Medicine, University of California at Los Angeles, Los Angeles, California

## Abstract

Substance P analogues, including [D-Arg<sup>1</sup>,D-Trp<sup>5,7,9</sup>,Leu<sup>11</sup>]SP (SPA) are broad-spectrum G protein–coupled receptor (GPCR) antagonists that have potential antitumorigenic activities, although the mechanism(s) are not completely understood. Here, we examined the effects of SPA in ductal pancreatic cancers that express multiple GPCRs for mitogenic agonists and also produce proangiogenic chemokines. Using HPAF-II, a well-differentiated pancreatic cancer cell line as our model system, we showed that SPA inhibited multiple neuropeptide-induced Ca<sup>2+</sup> mobilization, DNA synthesis, and anchorage-independent growth *in vitro*. SPA also significantly attenuated the growth of HPAF-II tumor xenografts in nude mice beyond the treatment period. Interestingly, SPA markedly increased apoptosis but moderately decreased proliferation marker, Ki-67 in the tumor xenografts implying additional mechanism(s) for the significant growth inhibitory effect observed *in vivo*. HPAF-II cells express ELR<sup>+</sup> CXC chemokines, including IL-8/CXCL8, which bind to CXCR2 (a member of GPCR superfamily) and promote angiogenesis in multiple cancers, including pancreatic cancer. SPA inhibited CXCR2-mediated Ca<sup>2+</sup> mobilization and blocked specifically IL-8/CXCL8-induced angiogenesis in rat corneal micropocket assay *in vivo*. A salient feature of the results presented here is that SPA markedly reduced tumor-associated angiogenesis in the HPAF-II xenografts *in vivo*. Our results show that SPA, a broad-spectrum GPCR antagonist attenuates tumor growth in pancreatic cancer via a dual mechanism involving both the antiproliferative and antiangiogenic properties. We conclude that this novel dual-inhibitory property of SPA could be of significant therapeutic value in pancreatic cancer, when used in combination with other antiproliferative and/or antiangiogenic agents. (Cancer Res 2005; 65(7): 2738-45)

## Introduction

Pancreatic ductal adenocarcinoma or pancreatic cancer is the most fatal gastrointestinal malignancy, with only 3% to 5% overall 5-year survival rate (1). Pancreatic cancer is mostly refractory to

current therapeutic regimens, rendering it nearly 100% lethal, and making it now the fourth leading cause of cancer death in both men and women (1). Thus, novel therapeutic strategies are urgently required, and these will most likely arise from a better understanding of the factors and signaling pathways that stimulate the proliferation of ductal pancreatic cancer cells (2).

Neuropeptide agonists and their cognate G protein–coupled receptors (GPCR) are increasingly implicated as autocrine/paracrine growth factors for multiple solid tumors including small cell lung cancer (SCLC), colon, breast, prostate, and pancreas (3, 4). We showed that pancreatic cancer cell lines express multiple functional GPCRs using Ca<sup>2+</sup> mobilization assay as indicator of productive ligand-receptor interactions (5). A variety of neuropeptides including neurotensin, bradykinin, and vasopressin stimulated DNA synthesis in multiple pancreatic cancer cell lines (5–7).<sup>5</sup> Furthermore, neurotensin strikingly increased protein kinase C–dependent mitogen-activated protein kinase activation, DNA synthesis, and colony formation in PANC-1 adenocarcinoma cells (6, 7). More recently, we showed that neurotensin acts synergistically with epidermal growth factor in promoting DNA synthesis and anchorage-independent growth of human pancreatic cancer cells, PANC-1 and MIAPaCa-2 (8). In addition to growth-promoting effects, GPCRs including CXCR2 are known mediators of angiogenesis (9). Chemokine receptors, including CXCR2 couple to Gα<sub>i</sub> and mediate multiple intracellular signaling pathways including angiogenesis in vascular endothelial cells (9). Pancreatic cancer cells produce CXCR2 ligands, ELR<sup>+</sup> CXC chemokines, which are potent promoters of angiogenesis in multiple solid cancers (9, 10). Consequently, antagonists capable of blocking the biological effects of multiple GPCR agonists (e.g., broad-spectrum GPCR antagonists) could provide a novel approach for the treatment of cancers, including pancreatic cancer that express GPCRs for mitogenic agonists and produce GPCR ligands that stimulate angiogenesis in a paracrine manner.

Substance P analogues, including [D-Arg<sup>1</sup>, D-Phe<sup>5</sup>, D-Trp<sup>7,9</sup>, Leu<sup>11</sup>]SP and [Arg<sup>6</sup>, D-Trp<sup>7,9</sup>, MePhe<sup>8</sup>]SP (SPG, refs. 6–11) block the biological effects of a broad range of GPCR agonists structurally unrelated to substance P in multiple cell types (11, 12). These broad-spectrum GPCR antagonists also inhibit the proliferation of SCLC cell lines in liquid culture, in soft agar, and as xenografts in nude mice (11, 12). Thus, SPG has recently completed a phase I clinical trial with minimal toxicity (facial flushing) and successfully blocked substance

**Note:** S. Guha and G. Eibl contributed equally to the work.

Supplementary data for this article are available at Cancer Research Online (<http://cancerres.aacrjournals.org/>).

**Requests for reprints:** Enrique Rozengurt, Department of Medicine, David Geffen School of Medicine, University of California at Los Angeles, 900 Veteran Avenue, Warren Hall Room 11-124, Los Angeles, CA 90095-1786. Phone: 310-794-6610; Fax: 310-267-2399; E-mail: [erozengurt@mednet.ucla.edu](mailto:erozengurt@mednet.ucla.edu).

©2005 American Association for Cancer Research.

<sup>5</sup> Unpublished observation.

P-induced vasodilatory effects *in vivo* with no dose-limiting toxicity (13). Recently, a more potent GPCR antagonist, [D-Arg<sup>1</sup>, D-Trp<sup>5,7,9</sup>, Leu<sup>11</sup>]SP or substance P antagonist (SPA), has been identified that also inhibited SCLC cell proliferation both *in vitro* and *in vivo* (14). However, it is not known whether SPA can block GPCR-mediated angiogenesis in tumors.

Given the fact that pancreatic cancer cells, including HPAF-II ductal adenocarcinoma cells express multiple GPCRs that mediate mitogenic signaling and produce proangiogenic ELR<sup>+</sup> CXC chemokines, including IL-8/CXCL8 (10, 15), we examined the effects of the potent broad-spectrum GPCR antagonist, SPA, in these cells growing *in vitro* and *in vivo*. We show that SPA blocked multiple neuropeptide-induced [Ca<sup>2+</sup>]<sub>i</sub> mobilization, decreased DNA synthesis, and anchorage-independent growth of HPAF-II cells *in vitro*. SPA also significantly attenuated the growth of established HPAF-II tumor xenografts *in vivo* beyond the treatment period and markedly increased apoptosis. Interestingly, SPA specifically and strikingly blocked IL-8/CXCL8-induced angiogenesis in the rat corneal micropocket assay and also significantly reduced tumor-associated angiogenesis of the HPAF-II xenografts *in vivo*. We conclude that SPA inhibits tumor growth via a dual mechanism involving both antimitogenic effects and a previously unrecognized antiangiogenic activity that could be of significant therapeutic values in pancreatic cancer.

## Materials and Methods

**Cell culture.** HPAF-II, obtained from American Type Culture Collection (Manassas, VA), is a well-differentiated line established from human ductal pancreatic adenocarcinoma. HPAF-II cells were grown in RPMI 1640 (Sigma, St. Louis, MO) with 10% fetal bovine serum (FBS) at 37°C in a humidified atmosphere containing 5% CO<sub>2</sub>. HEK-293 cells stably transfected with CXCR2 were grown in G-418 containing DMEM (Sigma) with 10% FBS at 37°C in a humidified atmosphere containing 5% CO<sub>2</sub>.

**Measurement of intracellular calcium.** Intracellular Ca<sup>2+</sup> concentration ([Ca<sup>2+</sup>]<sub>i</sub>) was measured with the fluorescent indicator fura-2 as previously described (5). Agonists and/or antagonists were added at various time points during recording.

**[<sup>3</sup>H]-Thymidine incorporation.** DNA synthesis was measured using [<sup>3</sup>H]-thymidine incorporation assay as previously described (6).

**Anchorage-independent cell growth.** Cells (2 × 10<sup>4</sup>) in either RPMI 1640 + 1% FBS, or RPMI 1640 + 10% FBS (positive control) were plated on tissue culture 12-well plates coated with polyhydroxyethylmethacrylate [poly-(HEMA)]. The growth of these cells in suspension was measured as previously described (8).

**Xenografts.** The HPAF-II xenograft was derived by implantation of 2 × 10<sup>7</sup> cells of the HPAF-II cell line into the right flanks of the male *nu/nu* mice. Histologic analysis confirmed the pathology of these xenografts.

**Animals.** Male *nu/nu* mice were maintained in specific pathogen-free facility at University of California at Los Angeles (UCLA). The UCLA Chancellor's Animal Research Committee approved all the animal experiments.

**Antitumor testing.** The animals were randomized into control and treated groups (12 mice per group) and were given punched ear tags to allow identification. Treatment was initiated when the tumors reached a mean diameter of 6 mm (initial experiment) and subsequently when the tumors reached a mean diameter of 2 mm, and the 1st day of treatment in both cases was designated as day 0. Tumor volume (*V*) was estimated as  $V = 2/3 \pi r^3$ , where *r* is the mean of the three dimensions (length, width, and depth). For injection into animals, [D-Arg<sup>1</sup>, D-Trp<sup>5,7,9</sup>, Leu<sup>11</sup>]SP (SPA) was dissolved in sterile water and was given once-daily peritumorally at 35 μg per g per day (50 μL/mouse) for 10 days.

**Ki-67 immunohistochemistry.** Cryostat sections (5 μm) were fixed in 95% ethanol, and stained with anti-Ki-67 (rabbit monoclonal clone SP6, NeoMarkers, Fremont, CA) antibody as previously described (16).

**Microvessel density.** Cryostat sections (5 μm) were fixed in acetone and stained with a rat anti-mouse CD31 monoclonal antibody (PharMingen, San Diego, CA) as previously described (17). Areas of greatest vessel density were then examined under higher magnification (100×) and counted. Any distinct area of positive staining for CD31 was counted as a single vessel. Results were expressed as the mean number of vessels ± SE per high-power field (HPF or 100×). A total of 20 HPFs were examined and counted from three tumors of each of the treatment groups.

**Human cytokine expression array assay.** The human cytokine array 5.1 was purchased from Ray Biotech (Norcross, GA) and used following the manufacturer's instructions (18).

**IL-8/CXCL8 ELISA.** Antigenic IL-8 was quantitated using a modification of a double-ligand ELISA method as previously described (19).

**Rat corneal micropocket assay.** *In vivo* angiogenic activity of the tumors was assayed in the avascular cornea of Long Evans rat eyes, as previously described (20).

**In situ terminal deoxynucleotidyl transferase-mediated nick end labeling assay.** Cryostat sections (5 μm) were fixed in 4% paraformaldehyde (in PBS, pH 7.4), and *in situ* terminal deoxynucleotidyl transferase-mediated nick end labeling (TUNEL) assay (Roche Diagnostics, Germany) was done as per the manufacturer's instructions described previously (21).

**Materials.** [<sup>32</sup>P] ATP (370 MBq/mL) was obtained from Amersham, plc. (Buckinghamshire, United Kingdom). Neurotensin, angiotensin-II, bombesin, bradykinin, vasopressin, cholecystokinin, RPMI 1640, and poly-(HEMA) were purchased from Sigma. [D-Arg<sup>1</sup>, D-Trp<sup>5,7,9</sup>, Leu<sup>11</sup>]SP (SPA) was obtained from Bachem, Inc. (Torrance, CA). All other reagents were of the purest grade available.

## Results

**[D-Arg<sup>1</sup>, D-Trp<sup>5,7,9</sup>, Leu<sup>11</sup>]SP prevents multiple G protein-coupled receptor agonist-induced increase in [Ca<sup>2+</sup>]<sub>i</sub>, DNA synthesis, and anchorage-independent growth in HPAF-II cells.** HPAF-II cells have been extensively used as a model system to study the effects of growth factors on the biological behavior of human pancreatic cancer cells (22–24). In addition, the histology sections of the HPAF-II tumors developed either in orthotopic or xenograft nude mice models closely resemble features of human pancreatic ductal adenocarcinoma (25). Thus, we used HPAF-II cells as our model system to study the effects of a broad-spectrum GPCR antagonist, [D-Arg<sup>1</sup>, D-Trp<sup>5,7,9</sup>, Leu<sup>11</sup>]SP (SPA), both *in vitro* and *in vivo*.

One of the earliest events induced by many GPCR agonists, including neurotensin, bombesin/gastrin releasing peptide, and vasopressin is a rapid phospholipase C<sub>β</sub>-mediated hydrolysis of phosphatidyl inositol-4,5-bisphosphate to produce the second messenger inositol-1,4,5-trisphosphate, which promotes mobilization of Ca<sup>2+</sup> from intracellular stores (5). In agreement with our previous results (5), addition of multiple GPCR agonists including angiotensin, neurotensin, bombesin/gastrin releasing peptide, bradykinin, cholecystokinin, and vasopressin induced rapid [Ca<sup>2+</sup>]<sub>i</sub> in HPAF-II cells (Fig. 1D). This substantiates that HPAF-II cells express functional GPCRs for multiple agonists. Representative tracings shown in Fig. 1A, B, and C, show that pretreatment with SPA potently blocked the transient increase in [Ca<sup>2+</sup>]<sub>i</sub> induced by neurotensin, bombesin, and vasopressin in HPAF-II cells. These results show that SPA, which is structurally unrelated to neurotensin, bombesin, and vasopressin can act as a broad-spectrum GPCR antagonist in the human pancreatic cancer HPAF-II cells.

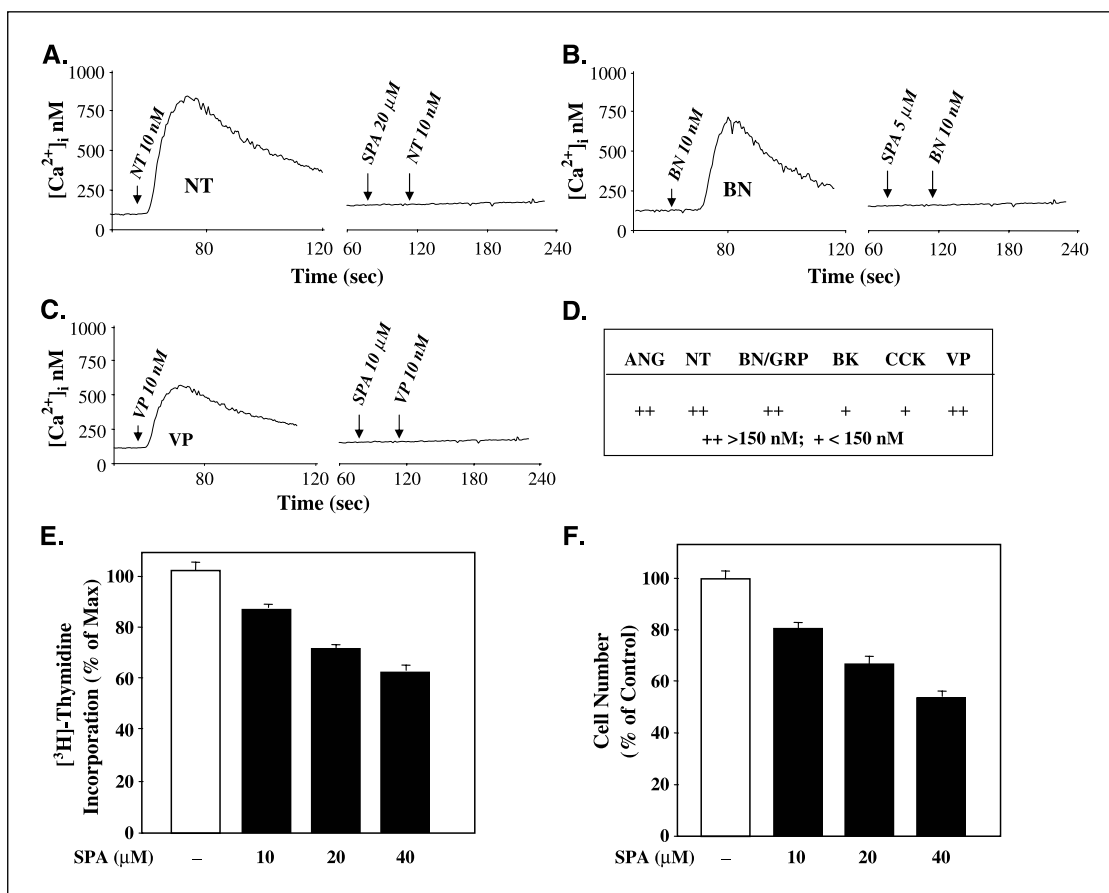


**Figure 1.** Effect of [D-Arg<sup>1</sup>,D-Trp<sup>5,7,9</sup>,Leu<sup>11</sup>]SP on multiple GPCR agonist-induced  $[Ca^{2+}]_i$ , DNA synthesis, and anchorage-independent growth of HPAF-II cells. **A**, cells grown on coverslips and loaded with fura-2/AM were stimulated with 10 nmol/L neurotensin (NT). Parallel cultures were pretreated with 20  $\mu$ mol/L of [D-Arg<sup>1</sup>,D-Trp<sup>5,7,9</sup>,Leu<sup>11</sup>]SP (SPA) and stimulated with 10 nmol/L of neurotensin. **B**, cells grown on coverslips and loaded with fura-2/AM were stimulated with 10 nmol/L bombesin (BN). Parallel cultures were pretreated with 5  $\mu$ mol/L of [D-Arg<sup>1</sup>,D-Trp<sup>5,7,9</sup>,Leu<sup>11</sup>]SP (SPA) and stimulated with 10 nmol/L of bombesin. **C**, cells grown on coverslips and loaded with fura-2/AM were stimulated with 10 nmol/L vasopressin (VP). Parallel cultures were pretreated with 10  $\mu$ mol/L of [D-Arg<sup>1</sup>,D-Trp<sup>5,7,9</sup>,Leu<sup>11</sup>]SP (SPA) and then stimulated with 10 nmol/L of vasopressin. Representative of three or more independent experiments. **D**, table depicts summary of  $[Ca^{2+}]_i$  responses to angiotensin (ANG), neurotensin (NT), bombesin/gastrin releasing peptide (BN/GRP), bradykinin (BK), cholecystokinin (CCK), and vasopressin (VP) in HPAF-II cells. ++, strong response (>150 nmol/L); +, weak response (<150 nmol/L). **E**, cells grown in 1% FBS were incubated with indicated amounts of [D-Arg<sup>1</sup>,D-Trp<sup>5,7,9</sup>,Leu<sup>11</sup>]SP (SPA; black column) or an equivalent amount of (-) solvent (white column) for 16 hours at 37°C. Cells were pulse-labeled with  $[^3H]$ -thymidine (0.25  $\mu$ Ci/mL), and the radioactivity incorporated into acid-soluble pools was counted in a scintillation counter as described in Materials and Methods. Representative plot from one experiment (four plates per condition). Similar results were obtained in three independent experiments. Bars,  $\pm$ SE. **F**, single-cell suspension of HPAF-II cells was plated in poly-(HEMA)-coated dishes at a density of  $2 \times 10^4$  cells per dish. Next day, SPA (black column) at indicated concentrations or equivalent amount of (-) solvent (white column) was added and the cells were incubated for 14 days as described in Materials and Methods. Cell count was determined from four plates per condition using a Coulter Counter. Columns, mean number of cells in four separate dishes expressed as the percentage of the solvent control (-); bars,  $\pm$ SE. Representative plot from one experiment. Similar results were obtained in two independent experiments.

Pancreatic cancer cells, including HPAF-II produce mitogenic GPCR ligands, which can promote proliferation in an autocrine/paracrine manner (26). As a first step to determine the mechanisms underlying the direct antiproliferative properties of SPA, we examined its effects on the incorporation of  $[^3H]$ -thymidine into DNA of HPAF-II cells. Confluent cultures of HPAF-II cells grown in medium containing 10% FBS were washed and transferred to fresh medium containing 1% FBS. To start the experiment, SPA at defined concentrations or solvent was added to parallel cultures for 16 hours and pulse labeled for 6 hours with  $[^3H]$ -thymidine. As shown in Fig. 1E, treatment with increasing concentrations of SPA reduced the DNA synthesis of HPAF-II cells in a concentration-dependent fashion.

Next, we investigated whether SPA could block the proliferation of HPAF-II cells growing in an anchorage-independent fashion, a hallmark of transformed cells. To test this possibility, single cell suspensions of HPAF-II cells were plated in medium

containing 1% FBS and SPA or solvent on culture dishes coated with poly-(HEMA), which prevents adhesion of the cells to the substratum. As illustrated in Fig. 1F, addition of increasing doses of SPA significantly inhibited (by 50%) HPAF-II cell numbers after 14 days of incubation. Our results show that SPA directly attenuates the proliferation of HPAF-II cells *in vitro*.

**Effect of [D-Arg<sup>1</sup>,D-Trp<sup>5,7,9</sup>,Leu<sup>11</sup>]SP on growth of HPAF-II tumor xenografts in nude mice.** Based on the antiproliferative effect of [D-Arg<sup>1</sup>,D-Trp<sup>5,7,9</sup>,Leu<sup>11</sup>]SP (SPA) *in vitro*, we next examined whether SPA could inhibit pancreatic cancer growth using HPAF-II tumor xenografts in nude mice. We used two distinct models to analyze the growth-inhibitory effect of SPA *in vivo*. Initially, we used an established tumor xenograft model to emulate the clinical scenario usually observed in pancreatic cancer. Specifically, we analyzed the effect of SPA in HPAF-II tumor xenografts that grew to an approximate volume of 150 mm<sup>3</sup>, which were generated by implanting  $2 \times 10^7$  cells in the right flanks of

the animals. Figure 2A shows that peritumoral injection of SPA at 35  $\mu\text{g}$  per g per day for 10 days in the established HPAF-II xenograft produced a significant inhibition of tumor growth ( $P < 0.05$ ) after 15, 20, and 25 days of initiating the 10-day treatment protocol. The representative H&E-stained sections of the xenograft tumors treated with vehicle show well-differentiated dysplastic ductal structures with characteristic arborization, network formation, dilated cystic spaces, and minimal to moderate desmoplastic changes (Fig. 2B, top). In contrast, a representative section of the treated HPAF-II tumors show well-differentiated dysplastic ductal structures in the periphery but prominent necrotic areas in the center (Fig. 2B, bottom).

Furthermore, we examined the effect of SPA in the xenograft model starting 3 days after the implantation of HPAF-II cells with approximate initial tumor volume of 50  $\text{mm}^3$ . This near-concurrent peritumoral administration of SPA simulates an *in vivo* model for tumors initiating metastatic processes. As shown in Fig. 2C, peritumoral injections of SPA virtually suppressed the growth of HPAF-II xenograft during the treatment period. Inhibition of tumor growth was maintained for at least 18 days after initiation of the SPA treatment (Fig. 2C, inset). Our results indicate that adminis-

tration of SPA significantly inhibits the growth of pancreatic cancer cells xenografted in nude mice.

**Effect of [D-Arg<sup>1</sup>,D-Trp<sup>5,7,9</sup>,Leu<sup>11</sup>]SP on Ki-67 expression and *in situ* apoptosis of HPAF-II tumor xenografts.** The results presented in Fig. 2 prompted us to investigate the mechanisms of the growth-inhibitory effects of [D-Arg<sup>1</sup>,D-Trp<sup>5,7,9</sup>,Leu<sup>11</sup>]SP (SPA) *in vivo* by analyzing the Ki-67 expression in the HPAF-II tumor xenografts. The expression of Ki-67 correlates well with other variables of cell proliferation including, thymidine labeling index, S-phase fraction, and mitotic count (27). Figure 3A illustrates representative tumor sections divided into central and peripheral zones labeled with Ki-67 SP-6 antibody (nuclear brown dots). Treatment with SPA significantly decreased Ki-67 labeling in the nonnecrotic tumor center (36%) compared with the periphery of the tumor (13%). Overall, SPA treatment only had a modest effect (22%) in reducing Ki-67 expression in HPAF-II tumor xenografts (Fig. 3A, inset).

Having documented that SPA decreased proliferation, we next examined whether SPA increased apoptosis in these tumor tissues. DNA degradation is considered a key event in apoptosis, resulting in cleavage of nuclear DNA into oligonucleosome-sized fragments

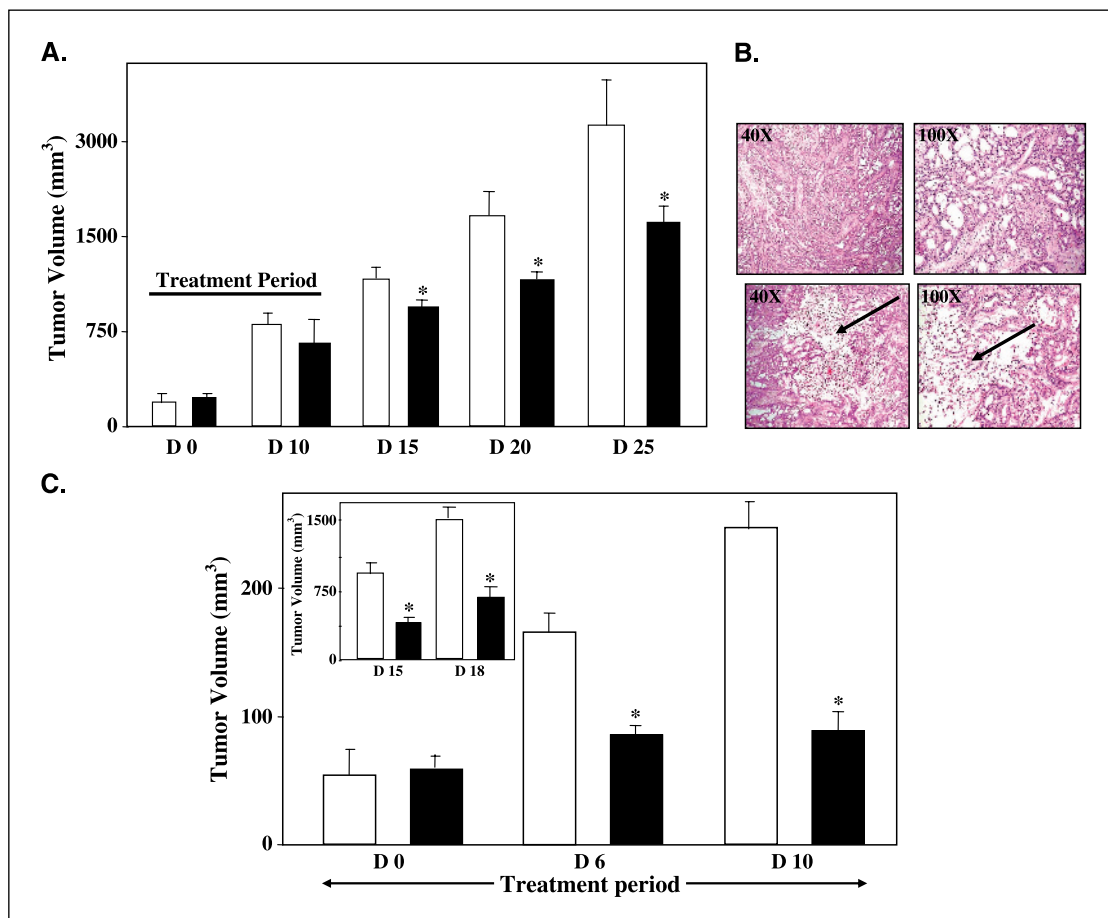


**Figure 2.** *In vivo* effect of [D-Arg<sup>1</sup>,D-Trp<sup>5,7,9</sup>,Leu<sup>11</sup>]SP on HPAF-II tumor xenografts. A, nude mice bearing single-flank tumors were randomized to receive once-daily peritumoral injection of sterile water (white column) or 35  $\mu\text{g}$  per g per day [D-Arg<sup>1</sup>,D-Trp<sup>5,7,9</sup>,Leu<sup>11</sup>]SP (SPA; black column) for 10 days and tumor volumes were measured at indicated time points as described in Materials and Methods; bars,  $\pm$ SE. At the start of the treatment, the median volume of the tumor xenografts was 150  $\text{mm}^3$ . B, representative H&E section of the HPAF-II tumor xenograft in 40 $\times$  magnification (top). Representative H&E section of the SPA-treated HPAF-II tumor xenograft in 40 $\times$  magnification (bottom). Arrow, points to central necrotic area noted in this section. C, nude mice bearing single-flank tumors were randomized to receive once-daily peritumoral injection of sterile water (white column) or 35  $\mu\text{g}$  per g per day of SPA (black column) for 10 days and tumor volumes were measured at indicated time points as described in Materials and Methods; bars,  $\pm$ SE. At the start of the treatment, the median volume of the tumor xenografts was 50  $\text{mm}^3$ . Inset, tumor volumes of the vehicle and SPA-treated xenografts 15 and 18 days after the initiation of the treatment. \*,  $P < 0.05$  versus control (Student's *t* test).

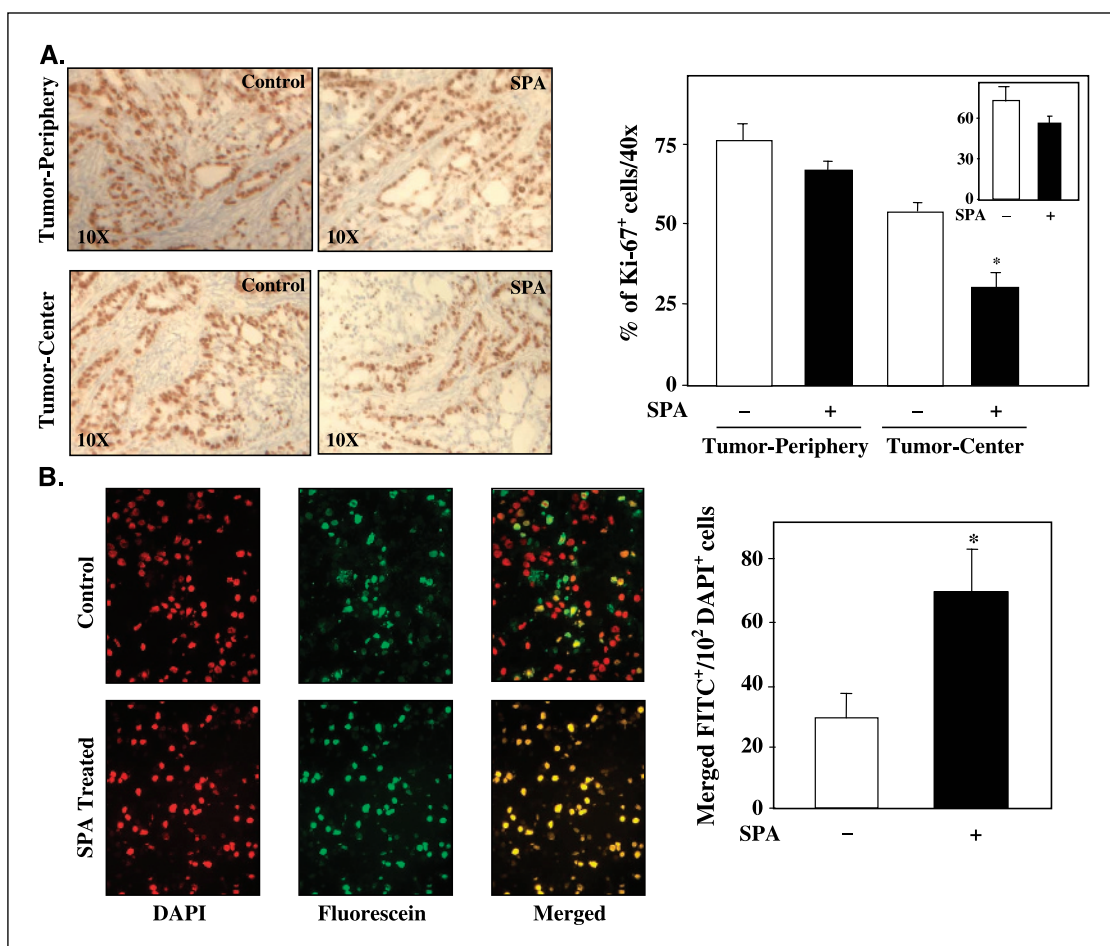


**Figure 3.** Effect of [D-Arg<sup>1</sup>,D-Trp<sup>5,7,9</sup>,Leu<sup>11</sup>]SP on Ki-67 expression and apoptosis *in vivo*. **A**, cryostat sections (5  $\mu$ m) were fixed in 95% ethanol, blocked with 0.3% H<sub>2</sub>O<sub>2</sub> in 0.1% sodium azide, and incubated in 1 mmol/L EDTA (pH 8.0) for retrieval of antigenic epitopes. The slides were next incubated with anti-Ki-67 monoclonal antibody (clone SP6) at 1:150 dilution as described in Materials and Methods. The sections were developed with 3',3'-diaminobenzidine tetrahydrochloride and counterstained with 1% hematoxylin solution as described in Materials and Methods. *Top*, Ki-67 expression in control (*left*) and [D-Arg<sup>1</sup>,D-Trp<sup>5,7,9</sup>,Leu<sup>11</sup>]SP (SPA)-treated (*right*) frozen sections from the tumor peripheries. *Bottom*, Ki-67 expression in control (*left*) and SPA-treated (*right*) frozen sections from the tumor centers. Mean number of Ki-67<sup>+</sup> cells per 100 cells counted in 10 fields under 40 $\times$  magnification (pooled from five mice per condition). *Columns*, % Ki-67<sup>+</sup> cells either in periphery or in central part of the tumor xenografts treated with (-) vehicle (*white column*) or SPA (*black column*). *Inset*, total % Ki-67<sup>+</sup> cells in the tumor xenografts treated with (-) vehicle (*white column*) or SPA (*black column*). Representative tumor section. *Tu-P*, tumor-periphery; *Tu-C*, tumor-center. \*,  $P < 0.05$  versus control (Student's *t* test). **B**, cryostat sections (5  $\mu$ m) of the HPAF-II tumor xenografts were fixed in 4% paraformaldehyde, blocked with 3% H<sub>2</sub>O<sub>2</sub> and permeabilized with 0.1% Triton X-100. *In situ* TUNEL assay was performed on these sections as described in Materials and Methods. Nuclei were counterstained with 4',6'-diamino-2-phenylindole (DAPI) and analyzed under a fluorescence microscope using an excitation wavelength of 480 nm and detection wavelength of 530 nm (*green*). *Left*, 4',6'-diamino-2-phenylindole-stained nuclei (pseudocolored *red* in Adobe Photoshop), TUNEL<sup>+</sup> cells (*green*), and merged (*yellow*) pictures of control or SPA treated HPAF-II sections. Number of merged FITC<sup>+</sup> cells/100 DAPI<sup>+</sup> cells in control (*white column*) or SPA treated (*black column*) tumor xenografts. *Columns*, mean values; *bars*,  $\pm$ SE. \*,  $P < 0.05$  versus control (Student's *t* test).

(28). We detected DNA strand breaks *in situ* by TUNEL assay on frozen sections of the HPAF-II xenografts. The fluorescein-labeled tissue was next mounted in a solution containing 4',6'-diamino-2-phenylindole, which stains the nuclei. As shown in Fig. 3B, SPA treatment markedly increased apoptosis (by 43%) compared with vehicle control in the tumor xenografts. Interestingly, exposure to SPA (1-20  $\mu$ mol/L) for 24 hours did not induce apoptosis in cultures of HPAF-II cells (data not shown). Thus far, our results suggest that SPA had a moderate growth-inhibitory effect *in vivo*. However, this does not explain the marked increase in apoptosis of the SPA-treated HPAF-II tumor xenografts.

**Effect of [D-Arg<sup>1</sup>,D-Trp<sup>5,7,9</sup>,Leu<sup>11</sup>]SP on IL-8/CXCL8 production in HPAF-II cells, IL-8/CXCL8-induced increase in [Ca<sup>2+</sup>]<sub>i</sub> in HEK-293-CXCR<sup>2+</sup> cells, IL-8/CXCL8-induced angiogenesis and tumor-associated angiogenesis *in vivo*.** To further explain the significant increase in apoptosis and central necrosis observed in

[D-Arg<sup>1</sup>,D-Trp<sup>5,7,9</sup>,Leu<sup>11</sup>]SP (SPA) treated tumors, we investigated whether SPA could also block angiogenesis in the HPAF-II xenografts. Inhibition of angiogenesis could indirectly promote apoptosis without significantly affecting tumor cell proliferation (29). ELR<sup>+</sup> CXC chemokines share a common chemokine receptor, CXCR2 and strongly promote tumorigenesis in human NSCLC xenograft models in severe combined immunodeficient mice (9). Thus, we hypothesized that SPA, a broad-spectrum GPCR antagonist, could block the proangiogenic effects of ELR<sup>+</sup> CXC chemokines during tumorigenesis and correspondingly increased apoptosis of the tumor xenografts.

Initially, using a human cytokine microarray assay, we screened the expression profile of cytokines from serum-starved confluent HPAF-II cells. The microarray membrane was immobilized with capture antibodies against 79 different cytokines (Supplementary Fig. S5). The membranes were hybridized with 1 mL of

supernatant from SPA-treated (20  $\mu\text{mol/L}$ , for 16 hours), or vehicle-treated (control) HPAF-II cells. The corresponding proteins were detected by a mixture of detection antibodies and visualized by an enhanced chemiluminescence system. Although HPAF-II cells produce multiple ELR<sup>+</sup> CXC chemokines, we used IL-8/CXCL8 as the representative proangiogenic chemokine for the current study. As shown in Fig. 4A, left (circled), IL-8/CXCL8 expression was detected in control HPAF-II cells and was not diminished by SPA treatment. Subsequently, we confirmed by ELISA that HPAF-II cells produce IL-8/CXCL8 and increasing concentrations of SPA did not block the IL-8/CXCL8 production (Fig. 4A, right). Next, we observed that HPAF-II cells do not express CXCR2, both at the mRNA and protein levels (data not shown). Thus, our results show that SPA did not block the IL-8/CXCL8 production by the HPAF-II cells.

Previous studies have reported that a related broad-spectrum GPCR antagonist, [D-Arg<sup>1</sup>,D-Phe<sup>5</sup>,D-Trp<sup>7,9</sup>,Leu<sup>11</sup>]SP, binds to IL-8 receptors (CXCR1 and CXCR2) on human neutrophils (30), but the effect of SPA on CXCR2-mediated angiogenesis has not been explored in any system. Using IL-8/CXCL8 and CXCR2 as representative ELR<sup>+</sup> CXC chemokine and its corresponding receptor, respectively, we examined whether SPA could block CXCR2-mediated rapid signaling events in HEK-293 cells stably transfected with CXCR2. As shown in Fig. 4B, SPA completely abrogated the rapid increase in [Ca<sup>2+</sup>]<sub>i</sub> induced by IL-8/CXCL8 in this model system. This strongly suggests that the inhibitory effect of SPA on IL-8/CXCL8-mediated downstream signaling events is at the level of CXCR2, a known GPCR. Next, we investigated whether SPA could block IL-8/CXCL8 induced angiogenesis in the avascular cornea of Long Evans rat eyes. We also tested the effect of SPA on

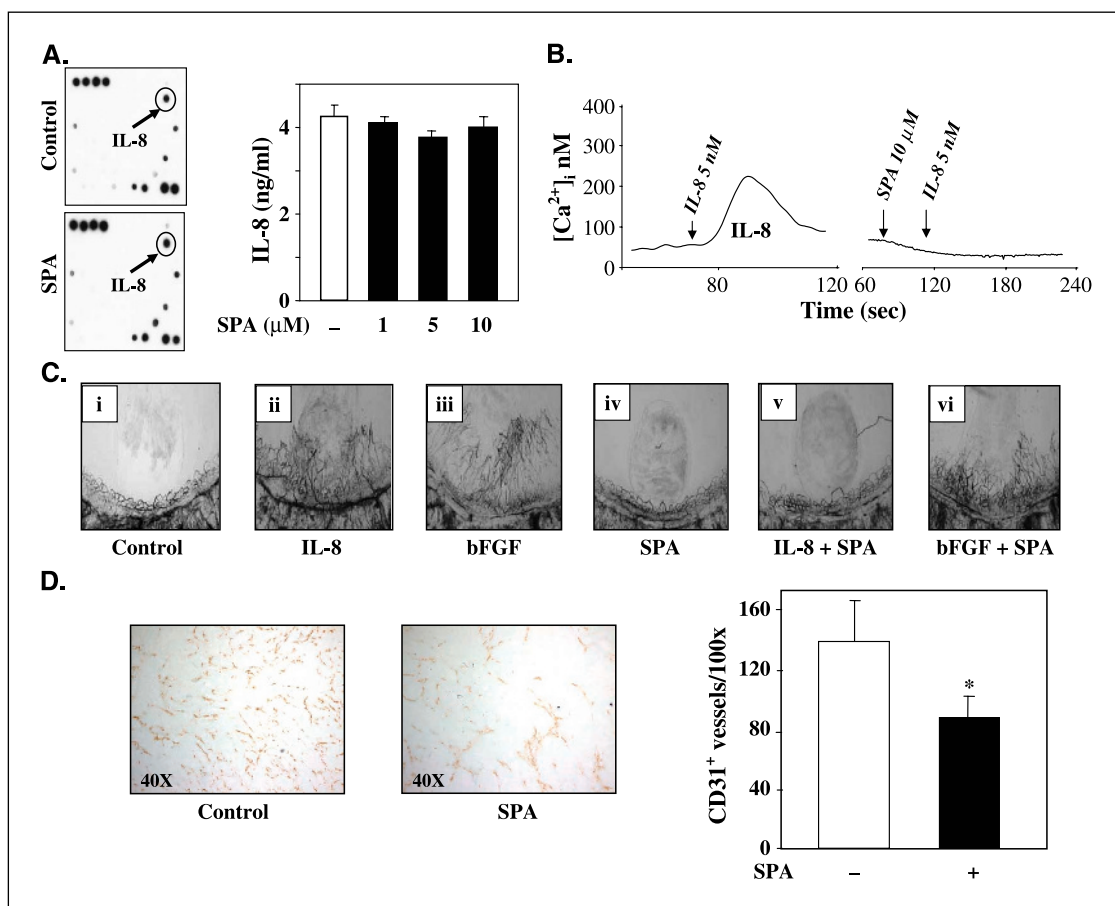


**Figure 4.** Effect of [D-Arg<sup>1</sup>,D-Trp<sup>5,7,9</sup>,Leu<sup>11</sup>]SP on IL-8/CXCL8 production in HPAF-II cells, IL-8/CXCL8-induced [Ca<sup>2+</sup>]<sub>i</sub> in HEK-293-CXCR2<sup>+</sup> cells, IL-8/CXCL8-induced angiogenesis, and tumor-associated angiogenesis *in vivo*. **A, left**, HPAF-II cells grown in serum-free condition were incubated with vehicle control (control) or 10  $\mu\text{M}$  [D-Arg<sup>1</sup>,D-Trp<sup>5,7,9</sup>,Leu<sup>11</sup>]SP (SPA) for 16 hours. Assay was performed with 1 mL of conditioned medium from each condition by following the manufacturer's protocol as described in Materials and Methods. Human cytokine array experiment was repeated twice with similar results. Representative experiment. **A, right**, HPAF-II cells ( $2 \times 10^4$ ) grown in serum-free condition were incubated with vehicle control (control) or SPA at indicated concentrations for 16 hours; 50  $\mu\text{L}$  of conditioned medium from the treated cells were used for IL-8/CXCL8 ELISA as described in Materials and Methods. IL-8/CXCL8 concentration either in (-) control (white column) or SPA treated (black column) HPAF-II cell supernatant. Columns, mean ( $n = 4$  per condition); bars,  $\pm$ SE. **B**, HEK-293-CXCR2<sup>+</sup> cells grown on coverslips and loaded with fura-2/AM were stimulated with 5 nmol/L IL-8/CXCL8. Parallel cultures were pretreated with 10  $\mu\text{mol/L}$  of [D-Arg<sup>1</sup>,D-Trp<sup>5,7,9</sup>,Leu<sup>11</sup>]SP (SPA) and then stimulated with 5 nmol/L IL-8/CXCL8. **C**, representative ( $n = 6$ ) photomicrographs of the corneal neovascularization responses to recombinant IL-8/CXCL8 (80 ng/pellet) or recombinant bFGF (50 ng/pellet) combined with vehicle control or 10  $\mu\text{mol/L}$  SPA and mixed with sterile hydon casting solution as described in Materials and Methods. **i-iii**, 50 $\times$  views, respectively, of corneas containing vehicle control, recombinant IL-8/CXCL8 or bFGF hydon pellets. **iv-vi**, 50 $\times$  views, respectively, of corneas containing SPA, recombinant IL-8/CXCL8 + SPA or bFGF + SPA hydon pellets. **D**, cryostat sections (5  $\mu\text{m}$ ) of the HPAF-II tumor xenografts were fixed in acetone, blocked with 2.5% BSA for 1 hour, and incubated with rat anti-mouse CD31 antibody (1:75) for 2 hours as described in Materials and Methods. Slides were then visualized with the Vectastain Elite ABC using 3,3'-diaminobenzidine as a chromogen. Images were obtained randomly on a Nikon Diaphot 300 microscope equipped with a Toshiba 3CCD camera. Representative control or SPA treated cryostat sections stained with CD31 (left). CD31<sup>+</sup> vessels were counted as described in Materials and Methods. Number of CD31<sup>+</sup> vessels/mm<sup>2</sup> either in control (white column) or SPA-treated (black column) tumor xenografts. Columns, mean values; bars,  $\pm$ SE. \*,  $P < 0.05$  versus control (Student's *t* test).

angiogenesis induced by basic fibroblast growth factor (bFGF), which acts through a tyrosine kinase receptor. Previous data showed that SPA does not interfere with the biological effects of ligands of tyrosine kinase receptors (31). Rat corneas were anesthetized and subsequently sterile Hydron pellets containing recombinant IL-8/CXCL8 (80 ng per pellet), or recombinant bFGF (50 ng per pellet) combined with vehicle control or SPA (10  $\mu$ mol/L) were implanted into an intracorneal pocket (1-2 mm from the limbus). Six days after implantation, the animals were perfused with colloidal carbon, the corneas were harvested and photographed. As shown in Fig. 4C, both IL-8/CXCL8 and bFGF potently increased neovascularization responses towards the implant. Interestingly, SPA markedly blocked IL-8/CXCL8-induced angiogenesis (four of six corneas) but not bFGF-induced angiogenesis (zero of six corneas) in the rat corneas (Supplementary Table S1). Thus, our results show that SPA significantly blocked IL-8/CXCL8-induced angiogenesis *in vivo* and the inhibitory action is at the level of the receptor, specific to the GPCR family.

Having established that SPA could block ELR<sup>+</sup> CXC chemokine-induced angiogenesis, we next examined whether SPA reduced microvessel formation in the tumor xenografts. It is well established that CD31 or platelet/endothelial cell adhesion molecule-1 (PECAM-1) is an adhesion molecule expressed on mature vascular endothelial cells and has been extensively used as a specific marker for microvessel formation (to calculate microvessel density) in the tumor sections (25). Thus, to detect tumor-associated neovascularization, we did immunohistochemistry on frozen sections from the HPAF-II xenografts with rat anti-mouse CD 31/PECAM-1 antibody. As shown in Fig. 4D, SPA treatment significantly reduced (by 44%) CD31<sup>+</sup> vessels/mm<sup>2</sup> in HPAF-II tumor xenografts. Taken together, our results suggest that SPA markedly reduced tumor-associated angiogenesis in the xenografts by acting on the host vascular endothelial cells. This is a novel property of broad-spectrum GPCR antagonist, SPA.

## Discussion

GPCRs that mediate agonist-induced signal transduction and cancer cell proliferation are attracting attention because they may provide potential targets for novel therapeutic interventions. HPAF-II pancreatic cancer cells, our model system in this study, express GPCRs for multiple mitogenic agonists and also produce proangiogenic ELR<sup>+</sup> CXC chemokines, including IL-8/CXCL8. Given the fact that GPCR agonists function as autocrine/paracrine growth factors for multiple cancers, including pancreatic cancer, we investigated whether the broad-spectrum GPCR antagonist, [D-Arg<sup>6</sup>, D-Trp<sup>7,9</sup>, Leu<sup>11</sup>]SP (SPA) could block growth of HPAF-II cells both *in vitro* and *in vivo*.

The results presented in this paper illustrate that SPA is a broad-spectrum GPCR antagonist that significantly reduced DNA synthesis and growth in suspension of the HPAF-II cells *in vitro*. SPA also attenuated growth of established HPAF-II tumor xenografts beyond the treatment period and reduced Ki-67 expression *in vivo*. However, SPA markedly increased apoptosis

*in vivo*. In addition, in contrast to studies showing that substance P derivatives can promote apoptosis of SCLC cells in culture (32), we did not observe any direct proapoptotic effect of SPA on HPAF-II cells *in vitro*. Interestingly, of the two HPAF-II xenograft models, we observed a prominent effect of SPA on the established tumor, which is quite akin to the clinical scenario in pancreatic cancer. In this model, SPA significantly attenuated growth beyond the treatment period, which could not be explained only by its antiproliferative property. Thus far, our results show that SPA not only has direct growth-inhibitory effects *in vitro* and *in vivo* but also has additional mechanism(s) to promote significant apoptosis and central necrosis observed *in vivo*. One of the mechanism could be inhibition of tumor-associated angiogenesis, as it was previously suggested that an established tumor predominantly depends on it for further growth (29).

A salient feature of this paper is that SPA significantly decreased tumor-associated angiogenesis and correspondingly increased apoptosis of HPAF-II xenografts *in vivo*. This is a novel finding for the group of broad-spectrum GPCR antagonists, including [Arg<sup>6</sup>, D-Trp<sup>7,9</sup>, MePhe<sup>8</sup>]SP or SPG (6-11), which is entering phase II clinical trial for SCLC. Our results showed that SPA specifically blocked IL-8/CXCL8 (member of ELR<sup>+</sup> CXC chemokines) and not bFGF-mediated corneal neovascularization *in vivo*. HPAF-II cells produce ELR<sup>+</sup> CXC chemokines, including IL-8/CXCL8 but do not express their corresponding receptor, CXCR2 (also a member of GPCR superfamily). CXCR2, predominantly expressed on the endothelial cells, is an important mediator of angiogenesis in multiple cancers. Here, we showed that SPA blocked CXCR2-mediated intracellular Ca<sup>2+</sup> mobilization. Thus, SPA blocked angiogenesis in HPAF-II tumor xenografts by inhibiting CXCR2-mediated signaling events in the host vascular endothelial cells. Taken together, this antiangiogenic property of SPA along with its growth-inhibitory effects could explain the pronounced and sustained growth attenuation observed in treated HPAF-II tumor xenografts.

In conclusion, our results raise the attractive possibility that treatment with SPA, a potent broad-spectrum GPCR antagonist, sustains growth inhibition *in vivo* by two different mechanisms: direct inhibition of cancer cell proliferation and by a previously unrecognized interference of the angiogenic properties of the HPAF-II tumor xenografts. The results provide a basis for novel noncytotoxic therapeutic strategies for the treatment of pancreatic cancer, a devastating disease with limited survival options.

## Acknowledgments

Received 9/7/2004; revised 12/10/2004; accepted 1/17/2005.

**Grant support:** Ronald S. Hirschberg Memorial Foundation for Pancreatic Cancer Research; NIH grant DK55003; and National Cancer Institute grant P50CA90388; Department of Medicine, David Geffen School of Medicine at UCLA specialty training and advanced research fellowship (S. Guha); and AGA Mentors' research scholar award (S. Guha).

The costs of publication of this article were defrayed in part by the payment of page charges. This article must therefore be hereby marked *advertisement* in accordance with 18 U.S.C. Section 1734 solely to indicate this fact.

We thank the members of the Rozengurt laboratory for many valuable discussions and Rodney Miller, M.D. (ProPath Laboratory, Inc., Dallas, TX) for valuable help with Ki-67 immunohistochemical staining.

## References

- Jemal A, Tiwari RC, Murray T, et al. Cancer statistics, 2004. *CA Cancer J Clin* 2004;54:8-29.
- Brand RE, Tempero MA. Pancreatic cancer. *Current Opinion in Oncology* 1998;10:362-6.
- Rozengurt E. Autocrine loops, signal transduction, and cell cycle abnormalities in the molecular biology of lung cancer. *Curr Opin in Oncol* 1999;11:116-22.
- Rozengurt E. Neuropeptides as growth factors for normal and cancer cells. *Trends Endocrinol Metab* 2002;13:128-34.
- Ryder NM, Guha S, Hines OJ, Reber HA, Rozengurt E. G protein-coupled receptor signaling in human ductal pancreatic cancer cells: neurotensin responsiveness and mitogenic stimulation. *J Cell Physiol* 2001;186:53-64.
- Guha S, Lunn JA, Santiskulvong C, Rozengurt E. Neurotensin stimulates protein kinase C-dependent

- mitogenic signaling in human pancreatic carcinoma cell line PANC-1. *Cancer Res* 2003;63:2379–87.
7. Guha S, Rey O, Rozengurt E. Neurotensin induces protein kinase C-dependent protein kinase D activation and DNA synthesis in human pancreatic carcinoma cell line PANC-1. *Cancer Res* 2002;62:1632–40.
  8. Kisfalvi K, Guha S, Rozengurt E. Neurotensin and EGF induce synergistic stimulation of DNA synthesis by increasing the duration of ERK signaling in ductal pancreatic cancer cells. *J Cell Physiol* 2005;202:880–90.
  9. Strieter RM, Belperio JA, Phillips RJ, Keane MP. CXC chemokines in angiogenesis of cancer. *Semin Cancer Biol* 2004;14:195–200.
  10. Shi Q, Abbruzzese JL, Huang S, Fidler IJ, Xiong Q, Xie K. Constitutive and inducible interleukin 8 expression by hypoxia and acidosis renders human pancreatic cancer cells more tumorigenic and metastatic. *Clin Cancer Res* 1999;5:3711–21.
  11. Langdon S, Sethi T, Ritchie A, Muir M, Smyth J, Rozengurt E. Broad spectrum neuropeptide antagonists inhibit the growth of small cell lung cancer *in vivo*. *Cancer Res* 1992;52:4554–7.
  12. Woll PJ, Rozengurt E. A neuropeptide antagonist that inhibits the growth of small cell lung cancer *in vitro*. *Cancer Res* 1990;50:3968–73.
  13. Clive S, Webb DJ, MacLellan A, et al. Forearm blood flow and local responses to peptide vasodilators: a novel pharmacodynamic measure in the phase I trial of antagonist G, a neuropeptide growth factor antagonist. *Clin Cancer Res* 2001;7:3071–8.
  14. Seckl MJ, Higgins T, Widmer F, Rozengurt E. [D-Arg<sup>1</sup>,D-Trp<sup>5,7,9</sup>,Leu<sup>11</sup>]substance P: a novel potent inhibitor of signal transduction and growth *in vitro* and *in vivo* in small cell lung cancer cells. *Cancer Res* 1997;57:51–4.
  15. Raut CP, Takamori RK, Davis DW, Sweeney-Gotsch B, O'Reilly MS, McConkey DJ. Direct effects of recombinant human endostatin on tumor cell IL-8 production are associated with increased endothelial cell apoptosis in an orthotopic model of human pancreatic cancer. *Cancer Biol Ther* 2004;3:7.
  16. Scott IS, Morris LS, Bird K, et al. A novel immunohistochemical method to estimate cell-cycle phase distribution in archival tissue: implications for the prediction of outcome in colorectal cancer. *J Pathol* 2003;201:187–97.
  17. Keane MP, Belperio JA, Xue YY, Burdick MD, Strieter RM. Depletion of CXCR2 inhibits tumor growth and angiogenesis in a murine model of lung cancer. *J Immunol* 2004;172:2853–60.
  18. Rhee SH, Keates AC, Moyer MP, Pothoulakis C. MEK is a key modulator for TLR5-induced interleukin-8 and MIP3 $\alpha$  gene expression in non-transformed human colonic epithelial cells. *J Biol Chem* 2004;279:25179–88. Epub 2004 Apr; 25176.
  19. Lane BR, Liu J, Bock PJ, et al. Interleukin-8 and growth-regulated oncogene alpha mediate angiogenesis in Kaposi's sarcoma. *J Virol* 2002;76:11570–83.
  20. Koch AE, Halloran MM, Haskell CJ, Shah MR, Polverini PJ. Angiogenesis mediated by soluble forms of E-selectin and vascular cell adhesion molecule-1. *Nature* 1995;376:517–9.
  21. Bennett MW, O'Connell J, O'Sullivan GC, et al. Fas ligand and Fas receptor are coexpressed in normal human esophageal epithelium: a potential mechanism of apoptotic epithelial turnover. *Dis Esophagus* 1999; 12:90–8.
  22. Singh AP, Moniaux N, Chauhan SC, Meza JL, Batra SK. Inhibition of MUC4 expression suppresses pancreatic tumor cell growth and metastasis. *Cancer Res* 2004;64: 622–30.
  23. Ebert M, Yokoyama M, Friess H, Kobrin MS, Buchler MW, Korc M. Induction of platelet-derived growth factor A and B chains and over-expression of their receptors in human pancreatic cancer. *Int J Cancer* 1995;62: 529–35.
  24. Eibl G, Brummer D, Okada Y, et al. PGE(2) is generated by specific COX-2 activity and increases VEGF production in COX-2-expressing human pancreatic cancer cells. *Biochem Biophys Res Commun* 2003;306:887–97.
  25. Hotz HG, Reber HA, Hotz B, et al. An orthotopic nude mouse model for evaluating pathophysiology and therapy of pancreatic cancer. *Pancreas* 2003;26: e89–98.
  26. Murphy LO, Abdel-Wahab YH, Wang QJ, et al. Receptors and ligands for autocrine growth pathways are up-regulated when pancreatic cancer cells are adapted to serum-free culture. *Pancreas* 2001;22:293–8.
  27. Klein WM, Hruban RH, Klein-Szanto AJ, Wilentz RE. Direct correlation between proliferative activity and dysplasia in pancreatic intraepithelial neoplasia (PanIN): additional evidence for a recently proposed model of progression. *Mod Pathol* 2002;15:441–7.
  28. Eibl G, Reber HA, Wente MN, Hines OJ. The selective cyclooxygenase-2 inhibitor nimesulide induces apoptosis in pancreatic cancer cells independent of COX-2. *Pancreas* 2003;26:33–41.
  29. Holmgren L, O'Reilly MS, Folkman J. Dormancy of micrometastases: balanced proliferation and apoptosis in the presence of angiogenesis suppression. *Nat Med* 1995;1:149–53.
  30. Jarpe MB, Knall C, Mitchell FM, Buhl AM, Duzic E, Johnson GL. [D-Arg<sup>1</sup>,D-Phe<sup>5</sup>,D-Trp<sup>7,9</sup>,Leu<sup>11</sup>]Substance P acts as a biased agonist toward neuropeptide and chemokine receptors. *J Biol Chem* 1998;273:3097–104.
  31. Sinnett-Smith J, Santiskulvong C, Duque J, Rozengurt E. [D-Arg(1),D-Trp(5,7,9),Leu(11)]Substance P inhibits bombesin-induced mitogenic signal transduction mediated by both G(q) and G(12) in Swiss 3T3cells. *J Biol Chem* 2000;275:30644–52.
  32. MacKinnon A, Sethi T. [D-Arg<sup>6</sup>, D-Trp<sup>7,9</sup>, Nme-Phe<sup>8</sup>]substance P (6-11) activates JNK and induces apoptosis in small cell lung cancer cells via an oxidant-dependent mechanism. *Methods Mol Med* 2003;74:299–307.

# Cancer Research

The Journal of Cancer Research (1916–1930) | The American Journal of Cancer (1931–1940)

## Broad-Spectrum G Protein–Coupled Receptor Antagonist, [D-Arg<sup>1</sup>,D-Trp<sup>5,7,9</sup>,Leu<sup>11</sup>]SP: A Dual Inhibitor of Growth and Angiogenesis in Pancreatic Cancer

Sushovan Guha, Guido Eibl, Krisztina Kisfalvi, et al.

*Cancer Res* 2005;65:2738-2745.

<b>Updated version</b>	Access the most recent version of this article at: <a href="http://cancerres.aacrjournals.org/content/65/7/2738">http://cancerres.aacrjournals.org/content/65/7/2738</a>
<b>Supplementary Material</b>	Access the most recent supplemental material at: <a href="http://cancerres.aacrjournals.org/content/suppl/2005/04/20/65.7.2738.DC1.html">http://cancerres.aacrjournals.org/content/suppl/2005/04/20/65.7.2738.DC1.html</a>

<b>Cited Articles</b>	This article cites by 31 articles, 13 of which you can access for free at: <a href="http://cancerres.aacrjournals.org/content/65/7/2738.full.html#ref-list-1">http://cancerres.aacrjournals.org/content/65/7/2738.full.html#ref-list-1</a>
<b>Citing articles</b>	This article has been cited by 14 HighWire-hosted articles. Access the articles at: <a href="http://cancerres.aacrjournals.org/content/65/7/2738.full.html#related-urls">http://cancerres.aacrjournals.org/content/65/7/2738.full.html#related-urls</a>

<b>E-mail alerts</b>	<a href="#">Sign up to receive free email-alerts</a> related to this article or journal.
<b>Reprints and Subscriptions</b>	To order reprints of this article or to subscribe to the journal, contact the AACR Publications Department at <a href="mailto:pubs@aacr.org">pubs@aacr.org</a> .
<b>Permissions</b>	To request permission to re-use all or part of this article, contact the AACR Publications Department at <a href="mailto:permissions@aacr.org">permissions@aacr.org</a> .